

# MECHANICAL PROPERTIES OF HA/PLLA COMPOSITES WITH BIMODAL PARTICLE DISTRIBUTION

T.Takayama<sup>1\*</sup>, M.Todo<sup>2</sup>, H.Ito<sup>1</sup>

<sup>1</sup> Department of Polymer Science and Engineering, Yamagata University, Yamagata, Japan,

<sup>2</sup> Research Institute for Applied Mechanics, Kyushu University, Fukuoka, Japan

\* Corresponding author([t-taka@yz.yamagata-u.ac.jp](mailto:t-taka@yz.yamagata-u.ac.jp))

**Keywords:** *Poly(L-lactic acid), particle size distribution, composites, mechanical properties*

## 1 General Introduction

Poly(L-lactic acid) (PLLA) has widely been used as a biomaterial for bone fixation devices in orthopedic and oral surgeries due to its bioabsorbability [1]. Recently, hydroxyapatite (HA) filled PLLA composites have been developed to improve the rigidity, bioactivity and degradation rate of the PLLA implants.

In the previous study, Todo et al. investigated the relationship between microstructure and fracture behavior of HA/PLLA composites with four different kinds of HA particles [2]. They found that the mode I critical energy release rate,  $G_{IC}$ , of micro-size HA/PLLA are higher than that of nano-size HA/PLLA. In addition, Takayama et al. investigated the relationship between mechanical properties and particle size distribution [3]. They found that the mechanical properties, such as bending strength and modulus, and The mode I critical J-integral,  $J_{in}$ , of HA/PLLA composites with both micro- and nano-size HA particles were higher than those of monomodal HA/PLLA composites. However the detail of the mechanisms were not been understood yet.

In the present study, HA/PLLA composites with both micro-size and nano-size HA particles were fabricated, and their mechanical properties such as bending properties were evaluated to assess the effect of bimodal particle distribution on those properties. The mode I critical J-integral,  $J_{in}$ , was also evaluated, and their fracture mechanism was characterized by scanning electron microscopy. The macroscopic fracture property was then correlated with the micro-mechanism of fracture.

## 2 Experimental

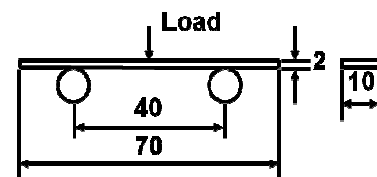
### 2.1 Materials

Two kinds of HA particles (Sangi Co. Ltd) with different shapes were used as filler. They are

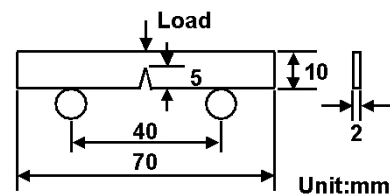
called on the basis of their shapes as micro-HA (5 $\mu$ m) and nano-HA (100nm), where the number in parentheses is the representative size. PLLA was used as matrix. HA/PLLA mixtures were prepared from the PLLA pellets and HA particles using a conventional melt-mixer by mixing for 20min at a rotor speed of about 50rpm at 190°C. Nine different compositions shown in Table 1 were chosen. HA plates of 140 $\times$ 140 $\times$ 2 mm<sup>2</sup> were fabricated from these mixture by re-melting at 190°C and pressed at 30MPa for 30min using a hot press. The plates were then quenched to room temperature using a water cooling system. Beam and Single edge notch bending (SENB) specimen as shown in Fig.1 were made from the HA/PLLA plates for 3-point bending tests and mode I fracture tests.

Table 1 Composition of HA/PLLA composites

Code	micro-HA(wt%)	nano-HA(wt%)
Micro	5,10,15	—
Nano	—	5,10,15
Bimodal (Micro:Nano)	2.5:2.5, 5:5, 7.5:7.5	



(a) Beam specimen



(b) SENB specimen

Fig.1 Geometry of specimens.

## 2.2 3-point bending testing

3-point bending tests were conducted at a loading-rate of 10mm/min by a servo-hydraulic testing machine. Bending strength and bending modulus were evaluated by complying with JIS K7171 [4].

## 2.3 Mode I fracture testing

Mode I fracture tests were conducted at a loading-rate of 1 mm/min by a servo-hydraulic testing machine. The mode I critical J-integral,  $J_{in}$ , were evaluated using the following formula:

$$J_{in} = \frac{\eta U_{in}}{W(B-a)} \quad (1)$$

where  $U_{in}$  is the energy corresponding the maximum load.  $B$  and  $W$  are the thickness and width of the SENB specimen, respectively.  $a$  and  $\eta$  are the initial crack length and the geometrical correction factor, equal to 2 for the standard SENB specimen. Fracture surfaces were examined by a scanning electron microscopy (SEM) to characterize the fracture mechanisms of HA/PLLA composites.

## 3 Results and Discussion

### 3.1 HA particle distribution

Figs.2 and 3 show FE-SEM micrographs of cryo-fracture surfaces of HA/PLLA composites with 15wt% of HA content and models showing dispersion of HA particles, respectively. In the case of Micro shown in Fig.2(a), agglomerations are invisible at this magnification, corresponding to good dispersion of the HA particles as shown in Fig.3(a). On the other hand, it is seen from Fig.2(b) that Nano has many agglomerations whose sizes are from about 15 to 50 $\mu$ m. This clearly indicates that the nano-HA particles agglomerate easily compared to the micro-HA particles as shown in Fig.3(b). Bimodal shows some agglomerations whose sizes are from about 5 to 15 $\mu$ m, which are much smaller than those of Nano. This clearly indicates that dispersibility of nano-HA is improved by dispersed micro-HA, as shown in Fig.3(c).

### 3.2 Bending properties

Typical Load-Displacement curves obtained from 3-point bending tests of HA/PLLA composites with 15wt% of HA content are shown in Fig.4(a). The maximum load of Bimodal is higher than that of Micro, and Nano exhibited lower maximum load than that of Micro. It is noted that sudden drop of

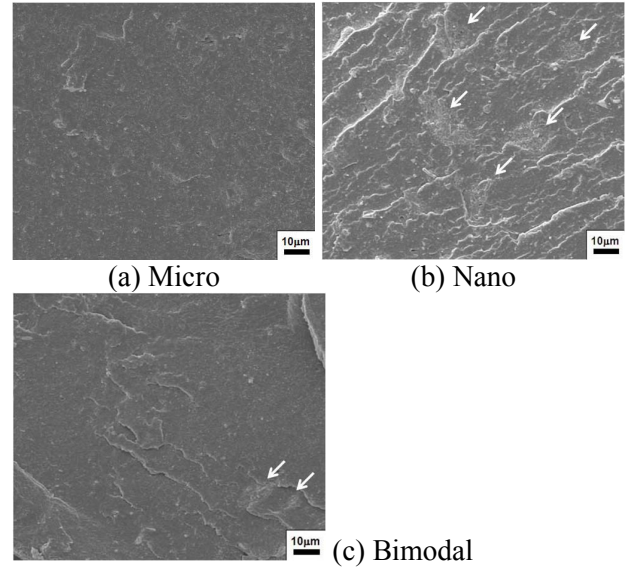


Fig.2 SEM micrographs of cryo-fractured surfaces of HA/PLLA composites with 15wt% of HA content.

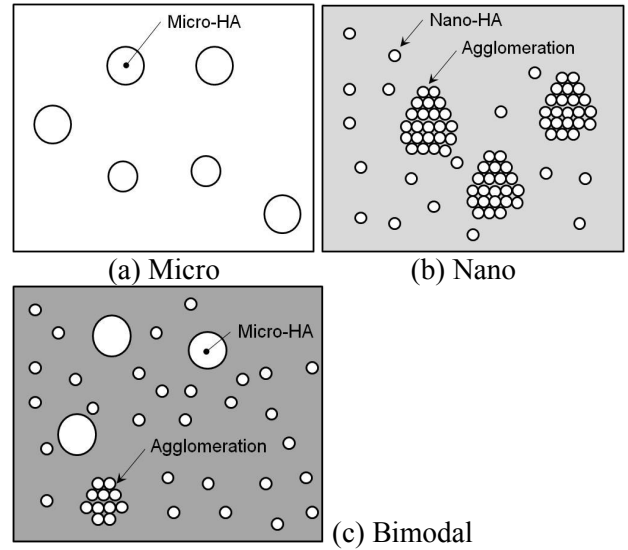


Fig.3 Models showing dispersibility of HA particles of HA /PLLA composites with different particle size distribution.

load after the peak indicated brittle fracture of the composites. Results of  $E$  and  $\sigma_f$  measurements are shown in Figs.4(b) and (c), respectively. Bimodal exhibited the highest  $\sigma_f$  value. Micro was next to Bimodal, and the difference between them was small. Nano was the lowest and much lower than those of Micro and Bimodal. Bimodal showed the highest value of  $E$ .  $E$  of Nano was similar to that of Micro. This result indicates that bimodal distribution of HA particles is more effective than monomodal

distribution for increase of  $E$  of neat PLLA ( $E$  of neat PLLA is about 4.0 GPa).

Lewis and Nielsen[5] showed that for particulate filled composites, the law of mixtures for the elastic modulus,  $E_c$ , of the composites is given by

$$\frac{E_c}{E_m} = \frac{1 + ABV_f}{1 - B\psi V_f} \quad (2)$$

where

$$A = \frac{7 - 5\nu_m}{8 - 10\nu_m} \quad (3)$$

and

$$B = \frac{E_f / E_m - 1}{E_f / E_m - A} \quad (4)$$

where  $V_f$  and  $E_f$  are volume fraction and elastic modulus of the filler, and  $\nu_m$  and  $E_m$  are the Poisson ratio and elastic modulus of the matrix.  $\psi$  depends on the maximum packing fraction  $\phi_m$  of the filler as follows:

$$\psi = 1 + \frac{1 - \phi_m}{\phi_m^2} V_f \quad (4)$$

For Micro under consideration,  $E_f$  and  $E_m$  are equal to 114GPa[6] and 4.0 GPa[7], respectively, and  $\nu_m$  and  $\phi_m$  are assumed to be 0.35 and 0.632, respectively. The theoretical value obtained from Eq.(2) is relatively similar to the experimental values for Micro as shown in Fig.4(c). It is however lower than the value for Nano and Bimodal. For nano-composites, it is well known that the elastic modulus is almost equivalent the value given by Halpin-Tsai equation[8] as shown as follows:

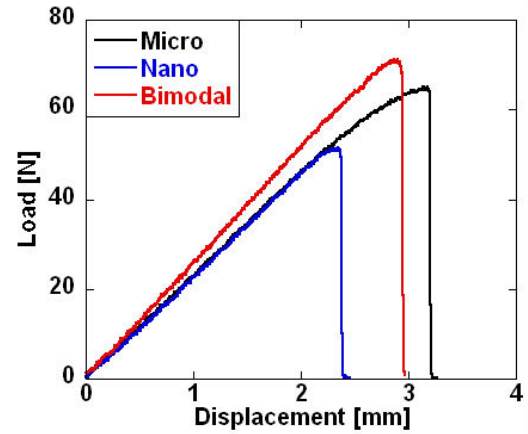
$$\frac{E_c}{E_m} = \frac{1 + ABV_f}{1 - B\psi V_f} \quad (5)$$

where

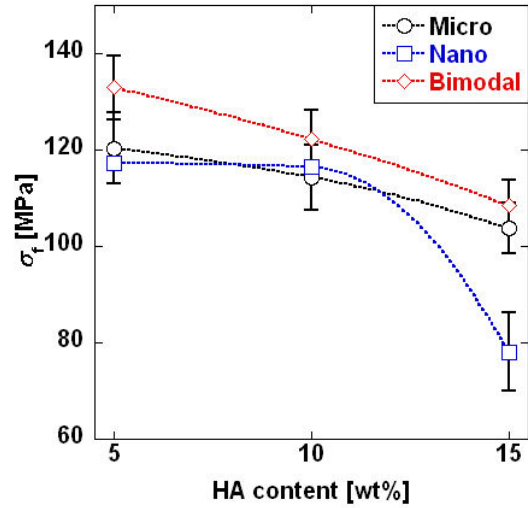
$$A = 2(L/D) \quad (6)$$

and

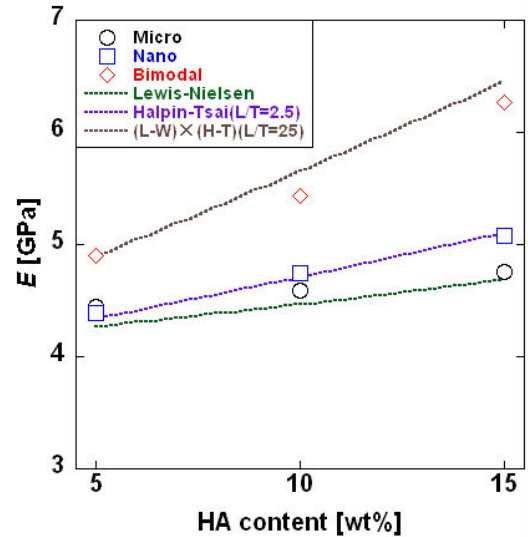
$$B = \frac{E_f / E_m - 1}{E_f / E_m - A} \quad (7)$$



(a) Load-displacement curves



(b) Bending strength



(c) Bending modulus

Fig.4 Bending properties of HA/PLLA composites obtained from 3-point bending tests.

where  $L/D$  is aspect ratio of filler. For Nano under consideration,  $L/D$  and  $\phi_m$  are assumed to be 2.5 and 0.82, respectively. The theoretical value obtained from Eq.(5) is relatively similar to the experimental values for Nano as shown in Fig.4(c). It is also however much lower than the value for Bimodal. On the above session, it has shown that dispersibility of nano-HA is improved by dispersed micro-HA as shown as Fig.3(c). It is corresponded that nano-HA of Bimodal disperses homogeneously such as Micro-HA compared to that of Nano. Thus, the elastic modulus for Bimodal can be considered as follows:

$$\frac{E_c}{E_m} = \alpha_{Micro} \times \alpha_{Nano} \quad (8)$$

where  $\alpha_{Micro}$  and  $\alpha_{Nano}$  are the relative modulus for dispersed Micro-HA and Nano-HA, respectively.  $\alpha_{Micro}$  are thought to be able to calculate by Eq.(2), because  $E$  of Micro is similar to the values calculated by Eq.(2). In addition,  $\alpha_{Nano}$  are thought to be able to calculate by Eq.(5). In the case of Bimodal,  $L/D$  is assumed to 25, because Nano-HA disperses homogeneously compared to Nano. The theoretical value obtained from Eq.(8) is relatively similar to the experimental values for Bimodal as shown in Fig.4(c). From these results, it is found that this improved modulus by the Nano- and Micro-HA mixing is due to improved dispersion of Nano-HA by mixing the Micro-HA.

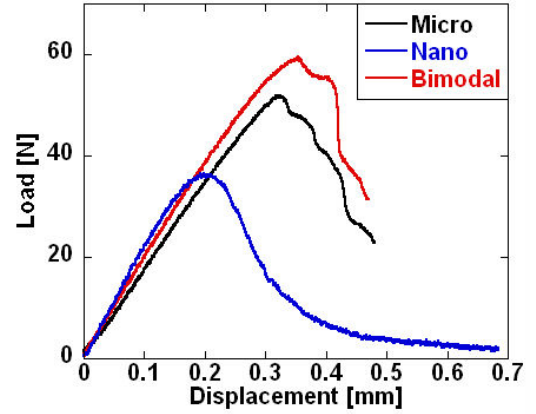
### 3.3 Mode I fracture property

Typical Load-Displacement curves obtained from mode I fracture tests of HA/PLLA composites with 15wt% of HA content are shown in Fig.5(a). The maximum load of Bimodal is higher than that of Micro, and Nano exhibited lower maximum load than that of Micro.

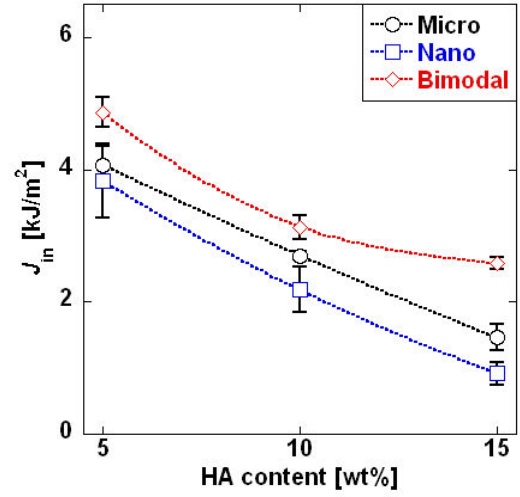
Dependences of particle distribution on the  $J_{in}$  of HA/PLLA with different HA content are shown in Fig.5(b). Bimodal exhibited the highest value of  $J_{in}$  at each HA content.  $J_{in}$  values of the Micro and Nano are much lower than that of Bimodal.  $J_{in}$  of Micro was lower than that of Bimodal, and Nano showed the lowest at each HA content.

### 3.4 Fracture mechanisms

SEM micrographs of HA/PLLA with different particle size distribution and models showing



(a) Load-displacement curves



(b) Fracture property,  $J_{in}$

Fig.5 Fracture properties of HA/PLLA composites obtained from mode I fracture tests.

fracture mechanisms of HA/PLLA are shown in Figs.6 and 7, respectively. In the case of monomodal, fracture surface of Micro is rough but a lot of voids with from about 5 to 10 $\mu$ m of diameter are visible. Those voids are created by debonding at interface between micro-HA particles and matrix under loading. Because those voids cause the localized stress concentration, those voids accelerate the initiation of crack growth as shown in Fig.7(a); therefore, lower the fracture energy compared to Bimodal. Fracture surface of Nano are smooth compared to those of any composites, corresponding to lowest the fracture energy, and rupture of agglomerations are visible as shown in white arrow in Fig.6(b). The existence of these agglomerations resulted in the reduction of the fracture energy because these are easily fractured due to weak



bonding between particles and such localized fracture becomes the initiation of fast global fracture of the composite material as shown in Fig.7(b).

On the other hand, fracture surface of Bimodal are invisible such voids and rupture of agglomerations, suggesting that mixing micro- and nano-HA can be reduced the void formation and be improved the dispersibility of nano-HA as shown in Fig.3(c). It is considered that those improvements are reduced initiation of crack growth, resulting in the highest fracture energy as shown in Fig.7(c).

#### 4. Conclusion

In this study, mechanical properties such as bending strength, modulus and J-integral at crack initiation of HA/PLLA composites with both micro-size and nano-size HA particles were investigated, and the following results were obtained:

- (1) Bending properties of Bimodal exhibited the highest. It is considered that dispersibility of nano-HA is improved by dispersed micro-HA.
- (2) J-integral at crack initiation of Bimodal also exhibited the highest. This reason is thought to be that mixing micro- and nano-HA can be reduced the void formation at the interface between matrix and micro-HA.

#### References

- [1] Leenslag JW, Pennings AJ, Bos RRM, Rozema FR, Boering J. "Resorbable materials of poly(L-lactide). VI. Plates and screws for internal fracture fixation." *Biomaterials*, Vol.8, pp.70-73, 1987.
- [2] Todo M, Park SD, Arakawa K, Takenoshita Y. "Relationship between microstructure and fracture behavior of bioabsorbable HA/PLLA composites" *Composites: Part A*, Vol.37, No.12, pp.2221-2225, 2006.
- [3] Takayama T, Todo M, Takano A, "The effect of bimodal distribution on the mechanical properties of hydroxyapatite particle filled poly(L-lactide) composites" *J Mech Behav Biomed Mater*, Vol. 2, No.1, pp.105-112, 2009.
- [4] JIS K7171. "Plastics—Determination of flexural properties" 1994.
- [5] Lewis TB, Nielsen LE, "Dynamic Mechanical Properties of particulate-filled composites" *J Appl Polymer Sci*, Vol.14, pp.1449-1471.
- [6] Gilmore RS, Kalz JL, "Elastic properties of apatites" *J Mater Sci*, Vol.17, pp.1131-1141, 1982.
- [7] Todo M, Takayama T, "Improvement of mechanical properties of Poly (L-lactic acid) by

blending of lysine triisocyanate" *J Mater Sci*, Vol.42, pp.4712-4715, 2007.

[8] Tsai SW, "Formulas for the Elastic Properties of Fiber-Reinforced Composites" *US Dept of Commerce Report*, AD834851, 1968.

[9] Halpin JC, "Stiffness and Expansion Estimates for Oriented Short Fiber Composites" *J Composite Mater*, Vol.3, pp.732-734, 1969.

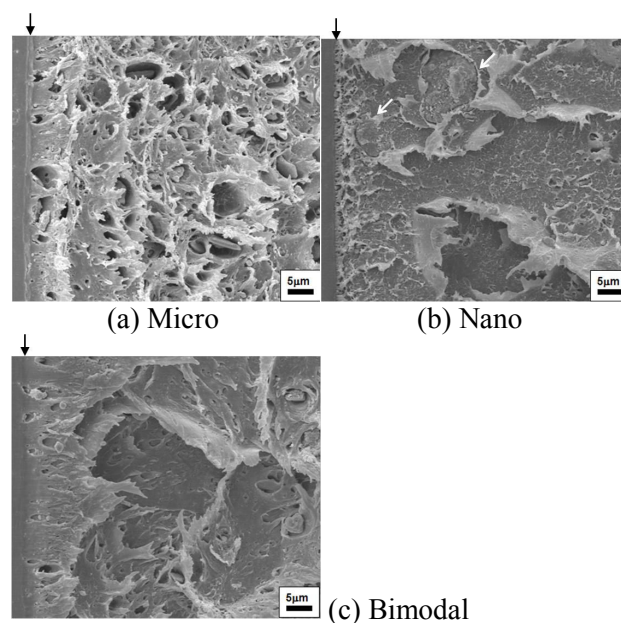


Fig.6 SEM micrographs of fracture surfaces obtained from mode I fracture tests of HA/PLLA composites with 15wt% of HA content.

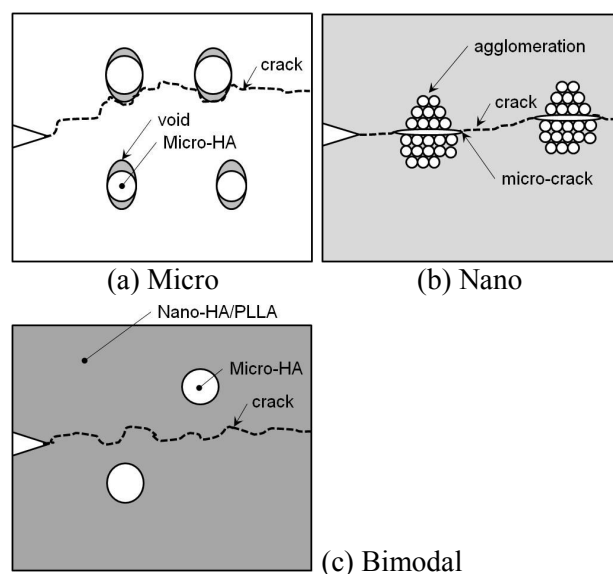


Fig.7 Models showing fracture mechanisms of HA/PLLA composites with different particle size distribution.